Ethanol Dehydration to Ethylene in a Stratified Autothermal Millisecond Reactor

A THESIS

SUBMITTED TO THE FACULTY OF THE GRADUATE SCHOOL

OF THE UNIVERSITY OF MINNESOTA

BY

Michael James Skinner

IN PARTIAL FULFILLMENT OF THE REQUIREMENTS

FOR THE DEGREE OF

Master of Science

Lanny D. Schmidt Advisor

Aditya Bhan, Advisor

April, 2011

Table of Contents

List of Tables

List of Figures

Chapter 1

Introduction

1.1 Next Generation Biomass to Biofuels Motivation

The United States has made the expansion of biofuel technology imperative. This can be seen in terms of federally funded research programs that have placed a large focus on renewable energy, and in recent policy decisions. For example, Hydrocarbons from Biomass was one of the topic choices for the National Science Foundation's 2009 Emerging Frontiers in Research and Innovation, and $400 million went into establishing the Advanced Research Projects Agency-Energy (ARPA-E), a national research program dedicated to fund research and development in technologies that have significant potential to increase domestic energy production and reduce greenhouse-gas emissions. In terms of policy, the Energy Independence and Security act (EISA) of 2007 sets domestic biofuel production standards through 2022.

The EISA sets a goal of 36 billion gallons per year of biofuel to be sold within the United States by 2022. The largest source of renewable fuel, ethanol, was produced in excess of 10 billion gallons in 2009.[1] However, commercially available biofuels such as ethanol or biodiesel require specific feed sources (starch, and lipids respectively) which represent only a small fraction of the total carbon in biomass, are politically unfavorable due to a food versus fuel argument, and are highly susceptible to feedstock prices.[2] These reasons demonstrate the need for a next generation biofuel that will use a cellulosic feedstock.

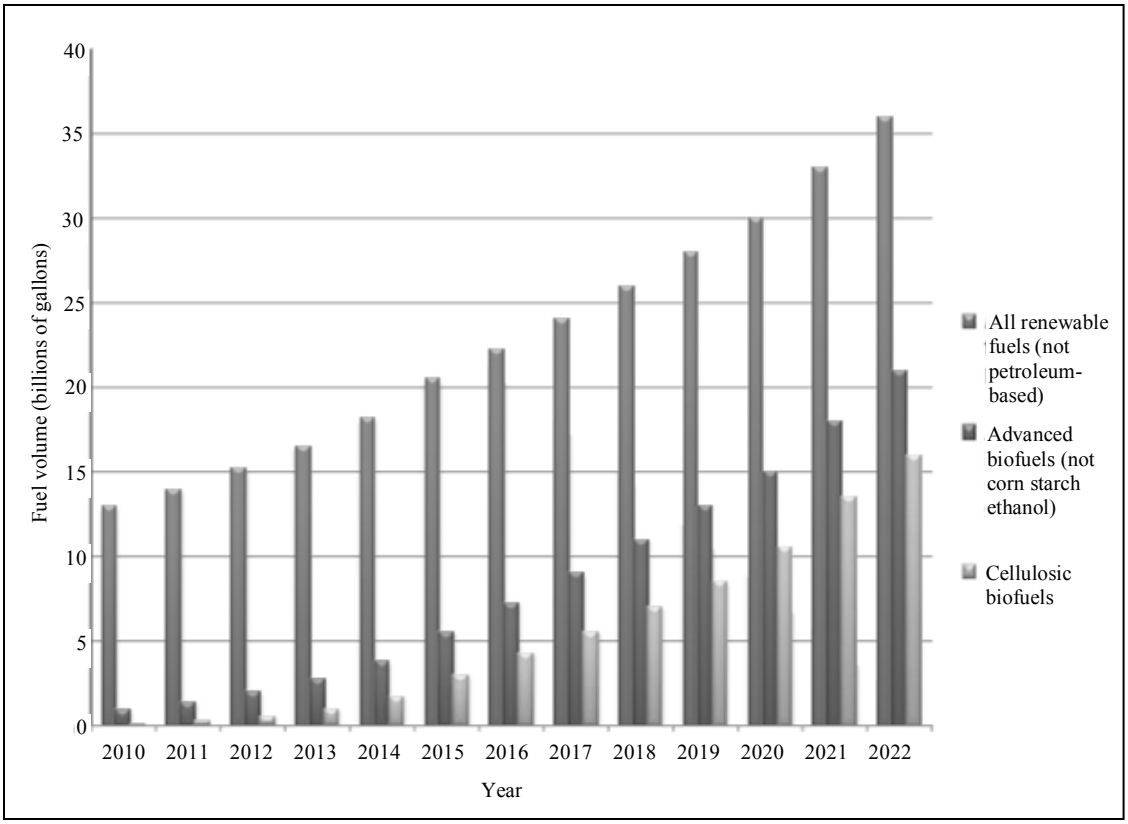

Figure 1.1 Energy Independence and Security Act of 2007 renewable fuel standards[2].

The need for cellulosic biofuel is acknowledged by the EISA, which sets a target of 15 billion gallons per year of cellulosic fuel by 2022.[2] For ethanol to remain as the best option for biofuel, cellulosic ethanol technology must be developed. However, there are significant disadvantages to proposed cellulosic ethanol processes. An NREL technoeconomic analysis of lignocellulosic biomass to ethanol via biomass gasificiation followed by alcohol synthesis shows that 40% of overall production costs would come from feedstock prices while an additional 20% would come from capital costs required to perform tar and gas cleanup.[3, 4] An economic examination of current and future biofuels predicts that total project investment for future biofuels such as corn based butanol or corn stover to ethanol by either a thermochemical or biochemical route require project

investments more than double that of existing starch ethanol biofuel plants due to the additional process steps needed to break down the more complex feedstocks.[5] Even if a biorefinery substitutes alcohol synthesis for a different fuel, such as synthesis gas production followed by Fischer-Tropsch synthesis of alkanes, these biorefineries will still be highly sensitive to feedstock prices, as well as to the large capital costs necessary to perform multiple process steps (gasification, gas cleanup, tar removal, and fuel synthesis).

1.2 Biomass to Biofuels Challenges

There are two fundamental challenges due to the nature of biomass that have so far prevented the development of a long term economically feasible and environmentally sustainable biomass to biofuel production facility. First, biomass is a diffuse resource with low energy density, and second, biomass contains significant quantities of oxygen. A next generation bioprocessing facility must address both of these challenges.

The energy density of biomass is less than half that of a barrel of oil. Perennial grasses and wood have energy densities of 15 and 21 MJ per kg respectively while crude oil has an energy density of 45 MJ per kg.[6,7] Additionally, unlike crude oil or coal, biomass is a highly distributed carbon source. Large point sources of crude oil allow for refineries to be built nearby major oil fields, while biomass will require harvesting over large areas of land. The low energy density and large land coverage demand that processing technologies utilize a majority of the carbon in biomass to ensure efficient use of land.

To minimize biomass harvesting and transportation costs, next generation biorefineries should consist of a network of smaller, distributed biomass processing facilities that are close to the biomass source. To achieve this, the processing facilities would need to reduce capital and operating costs by combining and eliminating process steps such as secondary reactors for tar cleanup and fuel synthesis. Instead of a gasification system, these biorefineries would need to make a liquid fuel directly from biomass.

1.3 Fast Pyrolysis Oils

By heating lignocellulosic materials in temperatures between 673-873 K at contact time between 30-1500 ms it is possible to form a liquid fuel, referred to as fast pyrolysis oil, that contains 70% of the energy content of the original biomass feed.[8,9] However, the physical properties of pyrolysis oil make it an impractical transportation fuel.[8,9,10, 11] The viscosities of pyrolysis oils can range from 35-1000 cP, making it unsuitable to pump through a pipeline or feed through a fuel injector. Pyrolysis oil has a pH range of 2-3, which can corrode metals and seals. Additionally, due to the hundreds of different compounds present in pyrolysis oil, it has a large volatility distribution. Attempts to distill pyrolysis oil have resulted in up to 50% wt of the material being turned into a residue that remains in the distillation column. Finally, the instability of pyrolysis oil as compounds react with themselves and with air results in physical properties that change over time. These problems stem from the oxygen content of pyrolysis oil, which is 35-40% wt oxygen, and is reflective of the large amount of oxygen present in lignocellulosic materials. Since lignocellulosic compounds account for over 75% dry

weight of corn stover and switchgrass, and over 90% in trees, the carbon in lignocelluloses must be used to form biofuels in order to maintain a high overall carbon efficiency.

Another processing challenge in pyrolysis oil formation is the significant tar and char formation that occurs in fluidized and circulating bed reactors using a lignocellulosic feedstock operating between 575 and 725 K reactors.[9,12] By using a Diebold Kinetic Model that uses first order kinetics to model pyrolysis oil as forming from an initial depolymerization step followed by a series-parallel network that can form pyrolysis vapors as well as char and tar, Cowdery and Reed calculated that in order to minimize char formation in cellulose pyrolysis below 0.01 wt%, 1 cm^3 cellulose particles must be heated at a rate of 10000 K/min.[12] Due to the low thermal conductivity of biomass, this works out to an approximate heat flux demand of 100 W per cm^2, a heat flux which either can not be achieved by current reactor technology or requires mechanisms such as radiation or ablation that are not feasible to implement in a practical biomass refinery.[9]

In summary, the two fundamental biomass processing challenges (expensive feedstock collection and high oxygen content) demand that a next generation biomass processing facility is a small-scale distributed refinery system that is capable of turning solid lignocellulosic biomass into a deoxygenated liquid fuel. Specifically, there are four requirements that must be met. To minimize capital and operating costs the facility must:

1. Reduce or eliminate process steps and streams such as secondary tar reactors, gas compression and clean up steps, high pressure systems, and recycle streams.
2. Be capable of processing a high throughput of biomass in a compact system.

In order to depolymerize biomass without forming coke or tar side products the reactor must:

3. Be able to transfer heat at a rate of at least 100 W per cm^2 to solid biomass.

In order to form a stable fuel with physical properties that allow it to be used as a transportation fuel the chemical processing method must:

4. Have a deoxygenation step capable of removing significant quantities of oxygen.

1.4 Multifunctional Reactors

Deoxygenation of biomass has been attempted by coupling pyrolysis reactors capable of decomposing biomass with zeolite catalysts capable of deoxygenating biomass.[8,13, 14]

Evans and Milne coupled pyrolysis of vegetable oil via an externally heated quartz tubular reactor with catalytic conversion of the resulting pyrolysis vapors over HZSM-5.[13, 15] Pyrolysis vapors were rapidly quenched and then sampled by a quadrupole mess spectrometer (sampling occurred less than 100 ms after pyrolysis to minimize secondary cracking and decomposition). Batch pyrolysis was performed by preheating helium to 773-863 K by an external furnace, then passing the helium over a boat contacting lipids. The helium gas pyrolyzed the lipids and the resulting vapor was then passed over a bed of HZSM-5 pellets at weight hourly space velocities between 1-6 g feed / g cat h and zeolite temperatures between 673-793 K. For all lipids studied, significant coking of the zeolite catalyst occurred, with coke formation estimates between 3-10%. For rapeseed oils, alkene and aromatic yields of approximately 70% and 20%

respectively were achieved, proving that a multi-functional reactor could be used to create hydrocarbons from lipids. In addition to testing rapeseed oil, whole rapeseeds were used as a biomass source as well. With whole rapeseeds, yields decreased significantly, to approximately 12% alkenes and 10% aromatics, indicating the difficulty in processing lignocellulosic materials.

More recently, the Evans and Milne reactor has been used by French and Czernik to study cellulose, lignin, and aspen wood catalytic pyrolysis between 673 and 873 K.[8] A mixture containing between 5:1 and 10:1 catalyst to biomass by weight was placed in a boat which was then exposed to a hot carrier gas. Forty different types of zeolites were used to examine hydrocarbon yield differences as a result due to pore size and structure as well as zeolites where different metals such as Co, Fe, or Ni were incorporated into the zeolite framework.

For the aspen wood pyrolysis without zeolite addition, most products were oxygenated compounds and no hydrocarbons were produced. With the addition of zeolites, the highest yield of hydrocarbons for catalytic pyrolysis was 16%, which occurred with a nickel-substituted ZSM-5 zeolite as well as a commercial zeolite, Zeolyst 8014. In general, ZSM-5 type catalysts including commercial, laboratory synthesized, and metal substituted zeolites had hydrocarbon yields between 10-16%. Coke formation for aspen wood pyrolysis was significant, with between 30-50% of coke formation occurring due to a combination of coke formation during the pyrolysis as well as during deoxygenation reactions on the zeolites.

Another attempt to combine zeolites with fast pyrolysis was performed by Diebold and Scahill who used an entrained-bed reactor to pryolyze 3 mm softwood

sawdust, then passed the pyrolysis vapors through a fixed bed reactor containing HZSM-5 catalyst.[14, 16] In this vortex reactor, pyrolysis occurs when sawdust particles entrained in steam contact the externally heated reactor walls. Wall contact time is increased in a vortex reactor compared to a tubular reactor due to the centrifugal forces that push sawdust particles against the reactor wall.[16] This reactor design, shown in figure 1.2, required a recycle loop and char removal to operate. Approximately 10% of the feed was converted to coke during pyrolysis, which was collected in the char receiver. Operations without a recycle loop demonstrated that approximately 30% of the feed would remain unconverted on the initial pass through the reactor. The pyrolysis vapor left the reactor and was fed to a fixed reactor bed with HZSM-5 catalyst maintained at 400 °C. Nonquantitative analysis by gas chromatography of liquid product obtained after sampling the catalytic reactor exit stream indicated that hydrocarbons in the form of methylated benzenes were produced.[14]

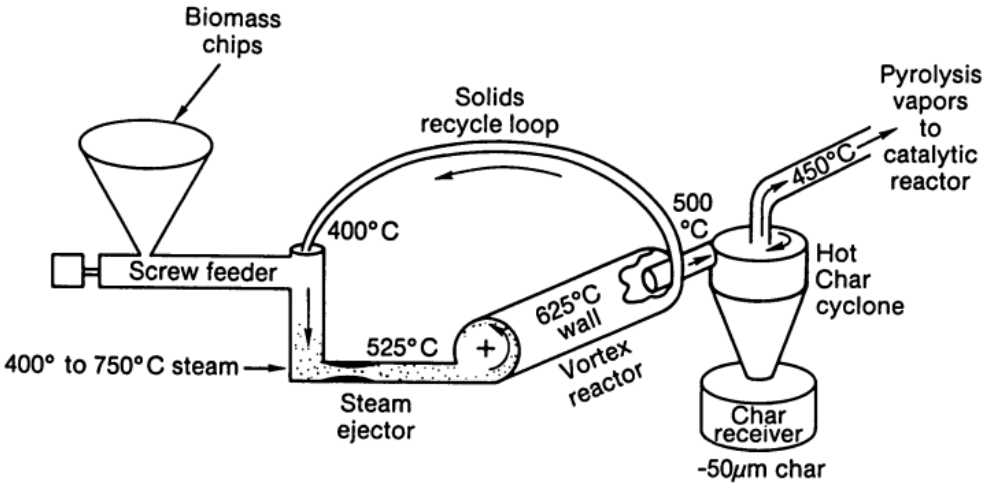

Figure 2.2 Entrained-bed vortex reactor for sawdust pyrolysis[16].

While these previous multifunctional reactor designs have demonstrated the ability to convert biomass to hydrocarbons via a pyrolysis, zeolite combination, they suffered from large amounts of coke formation, low hydrocarbon product yield, and data that was difficult to quantify due to the large amounts of compounds present.

1.5 Stratified Autothermal Millisecond Residence Time Reactor

In this research, a reactor capable of meeting all next generation biomass processing requirements has been designed and a proof of concept has been built and examined through autothermal ethanol dehydration experiments. The stratified autothermal millisecond residence time reactor, shown below in figure 1.3, is a two stage reactor that uses catalytic partial oxidation in the first stage to decompose biomass and a zeolite in the second stage to perform oxygen removal by dehydration reactions.

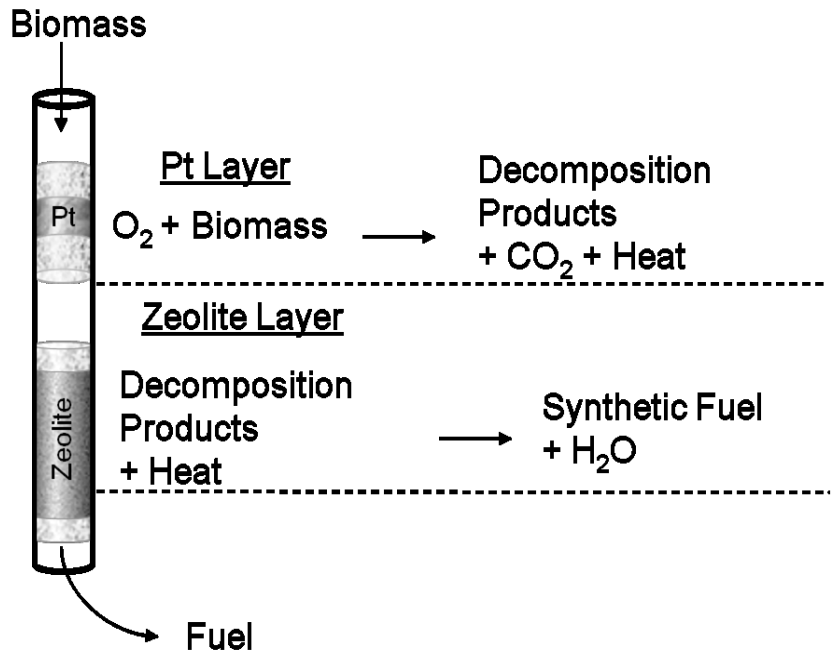

Figure 1.3 Short contact time multi layered autothermal reactor.

This reactor is essentially a short contact time catalytic partial oxidation reactor with a secondary zeolite catalyst stage incorporated downstream. Catalytic partial oxidation by short contact time reactors has been studied for over a decade by the Schmidt group. The work has covered gas, liquid, and solid feedstocks including methane, glycerol, and cellulose.[17,18,19] Reactor and catalyst parameters such as noble metal type and amount, support structure, and flowrate have been studied to identify how product conversion and selectivities change within the reactor as function of the fuel/oxygen ratio.[20,21,22]

Recently, Schmidt et al have demonstrated that such reactors are capable of achieving heat fluxes greater than 300 W per cm^2, meeting the requirement needed to minimize tar and char formation without adding any additional process heat.[23] Additionally, short contact time reactors operate in the millisecond contact time range, compared to unit operations used in petroleum refineries that operate in the second contact time range, this results in a 2-3 order of magnitude increase in reactor throughput.

Zeolite incorporation is necessary in the short contact time reactor to perform reactions that can not be achieved by noble metals such as deoxygenation reactions.[24] Zeolites are crystalline inorganic framework aluminosilicate materials that have pore sizes in the angstrom-nanometer range which allow for size and shape selectivity in catalysis. Additionally, zeolites are economical catalysts because they do not require expensive or exotic metals, and can be regenerated by flowing air or oxygen over the zeolite at high temperatures to remove any accumulated carbonaceous deposits.

In the short contact time multi layered autothermal reactor, solid biomass can be continuously co-fed with either oxygen or air. A carbon rich feed stream is needed to

ensure that only partial oxidation of the biomass occurs, generating C_1 products as well as releasing heat. The heat generated is used to depolymerize the remaining biomass as well as to drive the dehydration reactions in the zeolite downstream.

1.6 Summary

The work that follows demonstrates a small scale reactor system that combines multiple process steps (biomass decomposition and deoxygenation) into a single reactor. This reactor is capable of forming liquid hydrocarbons from in a continuous operation without requiring any additional process heat input and without forming significant char or tar while depolymerizing the biomass feed. Additionally, the short contact times in the reactor allow for higher feedstock throughputs than traditional petrochemical refineries. The result is a reactor that can be used as the basis for a small scale, distributed biomass to biofuel refinery.

Chapter 2

Ethanol Dehydration To Ethylene In A Stratified Autothermal Millisecond Residence Time Reactor

2.1 Overview

The concurrent decomposition and deoxygenation of ethanol was accomplished in a stratified reactor comprising of an upstream oxidation zone that contained Pt coated Al_2O_3 beads and a downstream dehydration zone consisting of H-ZSM-5 zeolite sheets deposited on Al_2O_3 monoliths with a 50-80 millisecond contact time. Ethanol conversion, product selectivity, and reactor temperature profiles were measured for a range of fuel: oxygen ratios for two autothermal reactor configurations: a parallel hydrogen-ethanol feed system and a series methane-ethanol feed system. Increasing the amount of oxygen relative to fuel resulted in a monotonic increase in ethanol conversion in both reaction zones. The majority of the converted carbon was in the form of ethylene, where the ethanol carbon-carbon bonds stayed intact while the oxygen was removed. These results demonstrate that noble metals can be successfully paired with zeolites to create a stratified autothermal reactor capable of removing oxygen from biomass model compounds in a compact, continuous flow system that can be configured to have multiple feed inputs depending on process restrictions.

2.2 Introduction

Biomass production is broadly distributed, and the low energy density of biomass implies there is an economic impasse to shipping large quantities of agricultural and

forest products to a few large refineries.[25] Additionally, cellulosic biomass contains nearly a one to one ratio of carbon to oxygen while hydrocarbon-derived gasoline contains no oxygen. These two challenges demand that technology for production of hydrocarbon fuels from biomass must be scalable and capable of removing oxygen from biomass.

Previously, we have reported a methodology for continuous processing of biomass involving thermal decomposition of cellulosic biomass on a catalytic surface in a millisecond contact time autothermal reactor which can be tailored to generate either synthesis gas or pyrolysis oil depending on reactor conditions.[10,19,26,27] This process has been shown to decompose microcrystalline cellulose and aspen wood chips to C_1 gases without producing coke in 30-70 ms residence time with Rh-Ce catalysts operating between 800-1000 K.[19,26] Millisecond contact time autothermal reactors are capable of converting a comparable amount of biomass as traditional solids gasification setups while being an order of magnitude smaller due to the high throughput rates which would allow for an infrastructure consisting of a distributed system of biomass processing facilities.[26]

While catalytic partial oxidation reactors can be used to decompose biomass, they have not yet been used to deoxygenate biomass, a critical challenge involved in the conversion of biomass to hydrocarbon fuels. To achieve this, a second stage containing a solid acid catalyst capable of deoxygenation reactions can be placed in series with the initial noble metal layer. Staged short contact time autothermal reactors have been demonstrated to alter both selectivity and conversion. For example, Klein examined staged catalytic methane partial oxidation reactors by incorporating an additional rhodium stage downstream of the initial oxidation that increased CO and H_2 selectivity as

well as methane conversion.[28] By incorporating multiple stages with different catalysts, it is possible to combine multiple reaction types at different temperatures. Specifically, in these experiments we are interested in combining partial oxidation and dehydration chemistries.

In our experiments, a stratified millisecond contact time autothermal reactor was used to convert ethanol, a surrogate biomass compound, to ethylene. Ethanol was chosen for these experiments as a model biomass compound because it contains C-H, C-O, and O-H bonds found in biomass. The stratified reactor was comprised of two sections: an upstream section with a noble metal where heat was generated by partial oxidation and a zeolite layer downstream that catalyzed dehydration reactions. Spatial separation of the two layers allowed the zeolite layer to operate at a lower temperature than the noble metal layer in order to reduce coke formation in the zeolite zone.[29]

Ethanol conversion, reactor temperatures, and product generation as a function of fuel: oxygen ratios were examined. We demonstrate that reactor temperature, and hence ethanol conversion in both reactor sections can be controlled by changing the amount of oxygen relative to the amount of fuel. A comparison of ethanol dehydration rates and product selectivities over the zeolite coated Al_2O_3 monoliths when used in the stratified reactor and when used in an isothermal reactor demonstrates the importance of limiting acetaldehyde formation, which can inhibit ethanol dehydration reactions over a zeolite.

Two autothermal configurations were examined for ethanol conversion and product generation: a parallel feed system where ethanol was co-fed with hydrogen upstream of the noble metal layer and a series feed system where ethanol was fed into the reactor downstream of the noble metal layer while methane was fed upstream of the

noble metal layer (Figure 2.1). This paper demonstrates that by using a series feed system that limits byproduct formation, ethylene production from ethanol doubled.

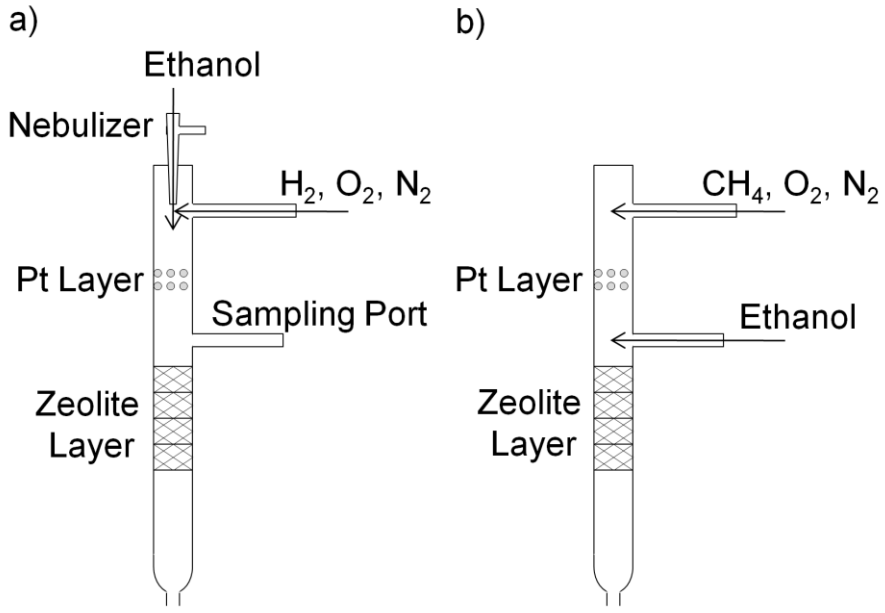

Figure 2.1. a) Autothermal stratified reactor with an ethanol-hydrogen co-feed. b) Autothermal stratified reactor with a methane feed upstream and an ethanol side feed (right).

2.3 Experiment

2.3.1 Isothermal Ethanol Conversion Experiments

Ethanol was fed by an ISCO Model 500D syringe pump (1.53×10^{-2} cm^3s^{-1}) into a concentric glass nebulizer made by Precision Glassblowing with nitrogen controlled by a mass flow controller operated by LabVIEW software (0.45 standard liters per minute, SLPM) where the ethanol was turned into an aerosol spray. The spray was injected into a horizontal quartz reactor tube. Additional nitrogen was fed into a reactor side arm so that the total flowrate was 3 SLPM. A diagram of the isothermal reactor is reported in the supporting information.

A tube furnace was used to maintain isothermal operation. The tube furnace was controlled by an Omega CSC32 benchtop controller connected to the middle thermocouple. Heating tape was wrapped around the ends of the reactor tube to prevent condensation in the reactor. A vacuum pump was used to draw a gaseous sample into a Hewlett Packard 5890 Series II gas chromatograph containing a Plot Q column connected to a thermal-conductivity and a flame-ionization detector used to analyze the composition of the effluent stream.

During the experiment, the pump flow rate as well as the reactor temperature was allowed to stabilize, then, three separate sample injections were analyzed before adjusting the experimental parameters to the next condition. Catalyst performance was examined for reactor temperatures between 523-723 K in 50 K temperature intervals. In between each temperature step, catalyst regeneration was performed by feeding a mixture of 20% oxygen 80% nitrogen at 0.5 SLPM into the reactor held at 773 K for one hour.

2.3.2 Autothermal Ethanol Dehydration Experiments

Ethanol, hydrogen, oxygen, and nitrogen were co-fed into the reactor at ethanol: hydrogen: oxygen (E:H:O) ratios varying between 6.4: 2: 1 and 1.7: 2: 1 at a constant flow rate of 3 SLPM in order to assess the effect of E:H:O ratios on reactor temperature, ethanol conversion, and product selectivities. Hydrogen was used as a sacrificial fuel to generate heat in combustion reactions upstream on the platinum coated Al_2O_3 beads.[30,31] The autothermal experiments used the same total flow rate and ethanol feed rate as the isothermal experiment. A stoichiometric ratio of hydrogen and oxygen was maintained throughout the initial autothermal experiments. The flow rate of hydrogen and oxygen

relative to ethanol was increased to increase the temperature in the reactor. After one hour on-stream, three gaseous samples were taken after the noble metal layer and after the zeolite layer for all conditions. In between each E:H:O change, catalyst regeneration was performed by feeding a mixture of 20% oxygen 80% nitrogen at 0.5 SLPM into the reactor held at 773 K for one hour to remove any accumulated carbonaceous deposits, followed by a mixture of 20% hydrogen 80% nitrogen at 0.5 SLPM into the reactor held at 773 K for one hour. A diagram of the autothermal reactor is reported in the supporting information.

A second set of autothermal experiments consisting of an upstream methane feed and an ethanol side feed was performed to examine the effect of methane catalytic partial oxidation at various CH_4/O_2 ratios on downstream ethanol conversion and product selectivities. Methane, oxygen, and nitrogen were fed upstream of the noble metal layer while ethanol was fed through a side port downstream of the noble metal layer. Methane was maintained constant at 1.08 SLPM while oxygen was varied so that CH_4/O_2 ratio varied between 1.4 and 2.2. The total feed input, including the ethanol side feed, was maintained at 3 SLPM by adjusting the nitrogen flow rate. Ethanol was vaporized by heating a 1.6 mm diameter steel tube coiled around a heating cartridge maintained at 373 K and then fed through the side port of the reactor by a 0.320 mm diameter fused silica capillary tube. The capillary tube was inserted into the side port so that the ethanol entered the reactor at the center. The ethanol was pumped into the system at the same rate as in the previous autothermal and isothermal experiments. An additional 80 ppi Al_2O_3 monolith was placed in the reactor between the ethanol feed point and the zeolite layer to promote mixing.

2.3.3 Catalyst Preparation

Zeolite

Approximately 0.2 g of H-ZSM-5 was deposited onto 10 mm long x 17 mm diameter 45 ppi Al_2O_3 monoliths as detailed in the supporting information section.

Platinum

Platinum was coated on 1.3 mm α-Al_2O_3 beads through incipient wetness impregnation. A solution of PtH_2Cl_6 (0.1799 g of a 13.14% wt solution) was deposited on to 2.28 g of α-Al_2O_3 beads, resulting in a 1% wt platinum coating. The beads were then dried overnight in a vacuum and then treated in a mixture of 20% H_2 in N_2 at 1 SLPM at 573 K for 3 hours.

2.4 Results and Discussion

2.4.1 Autothermal Ethanol Dehydration Experiments

Under autothermal experimental conditions with varying E:H:O ratio (range), all oxygen was consumed in the platinum section. Between 9-34% of ethanol was converted through heterogeneous and homogenous reactions in the noble metal section as dictated by E:H:O ratio. A larger amount of hydrogen and oxygen compared to ethanol resulted in more oxidation which generated more heat and thus higher operating temperatures downstream (Figure 2.2). Higher operating temperatures resulted in a higher selectivity to CO_2, consistent with reports for alcohol partial oxidation from Wanat who observed an increase in alcohol conversion to C_1 gases when the oxygen content was increased for fuel rich mixtures of alcohols, nitrogen, and air in a Rh-Ce catalytic partial oxidation reactor operating between 773-1173 K.[32]

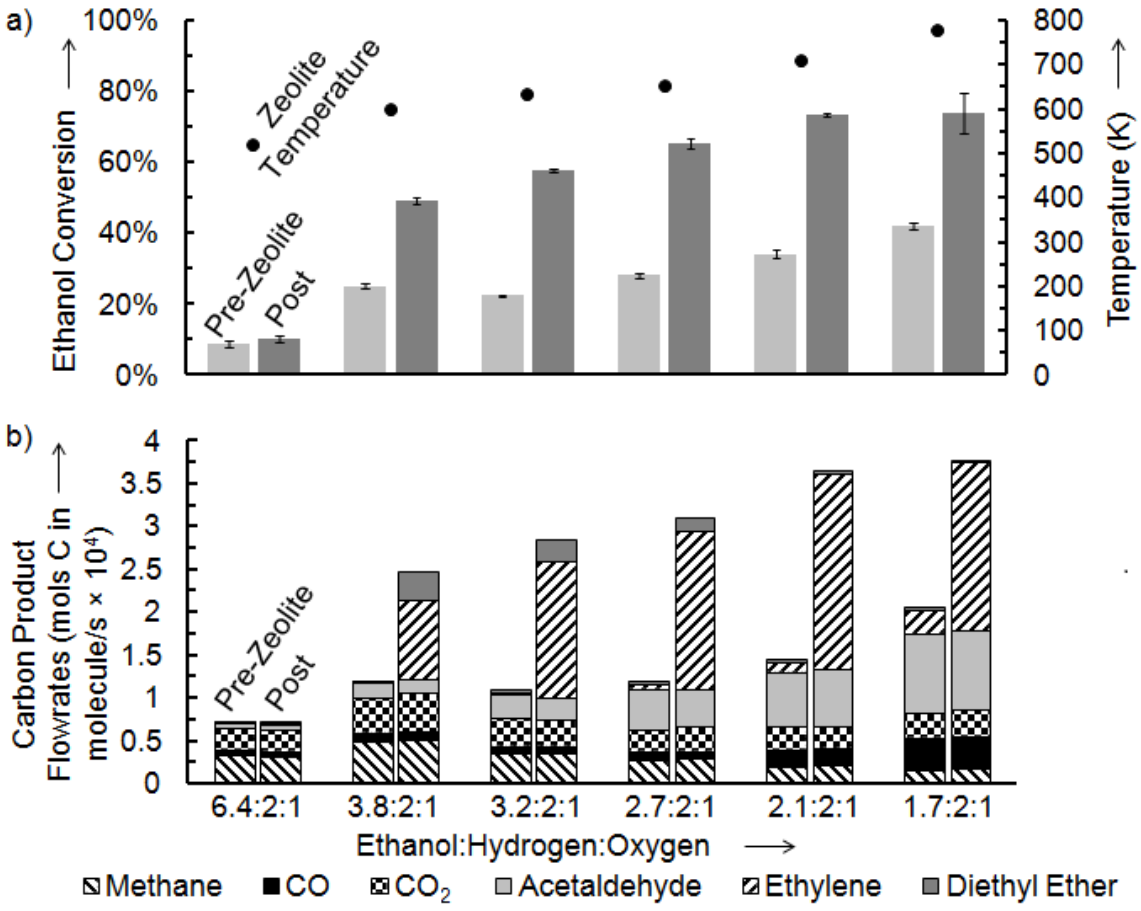

Figure 2.2 a) Autothermal ethanol conversion in the stratified reactor with an ethanol-hydrogen co-feed. Error bars on the ethanol conversion chart represent the 95% confidence interval. The temperature shown is for the middle zeolite-coated monolith. Pre-Zeolite Conversion (light gray), Post-Zeolite Conversion (dark gray), Zeolite Temperature (black circle). b) Carbon product flow rates. Diethyl Ether (dark gray), Ethylene (right slash), Acetaldehyde (light gray), CO_2 (checkered), CO (black), Methane (left slash). The total overall input into the reactor was maintained at 50 cm^3/s standard conditions. Ethanol was pumped as a liquid at 1.53×10^{-2} cm^3/s and fed to the reactor through a nebulizer. The noble metal section contained approximately 20 mg of platinum coated on Al_2O_3 beads. Each of the four Al_2O_3 monoliths in the zeolite section was coated with approximately 200 mg of H-ZSM-5. The zeolite and noble metal catalyst maintained operation at a steady state over the 1 hour duration for sampling under autothermal conditions.

Along with heat, ethanol oxidation and decomposition products (carbon monoxide, carbon dioxide, methane, and acetaldehyde) were generated in the platinum section as shown in figure 2.2. The carbon products obtained in the platinum layer can be explained by an ethanol decomposition scheme where ethanol is catalytically converted to acetaldehyde, which then decomposes to CO and CH_4 through an acetyl intermediate that can undergo decarbonylation to form CO and a methyl species as reported by Wilson

et al. in a fast XPS and TDP study of ethanol on Pt{1 1 1} ramping from 150-850 K.[33] CO_2 formation occurred through combination of CO oxidation on platinum as has been demonstrated by Hendriksen et al. during a scanning tunneling microscopy study of Pt {1 1 0} at 5×10^4 Pa and 425 K where Pt was observed to switch between metallic and oxidic states as a function of CO and O_2 pressures while effluent gases were monitored by a mass spectrometer, and through water gas shift as demonstrated by Wheeler et al. during autothermal CO conversion studies over Pt catalysts operating between 673-1273 K.[28,34,35,36]

The product flowrates for the Pt catalyzed reactions shown in figure 2.2 provide further evidence for methane and CO generation occurring through decarbonylation of an acetyl intermediate. At higher E:H:O conditions which cause lower reactor temperatures, there is a near 1:1 correlation between the total amount of carbon in CO and CO_2 versus carbon in CH_4. As the E:H:O decreases, the temperature increases, and the CO + CO_2 / CH_4 ratio increases. This can be explained by the consumption of methane through catalytic partial oxidation on platinum to form synthesis gas as first demonstrated by Hickman and Schmidt.[17]

In the zeolite section of the reactor, in some cases over 50% of the remaining ethanol was converted into dehydration products (ethylene and diethyl ether) as seen in figure 2.2. The products generated in the platinum section passed through the zeolite section without reacting as demonstrated by the unchanged flowrates of acetaldehyde, CO_2, CO, and methane reported in figure 2.2. Small amounts of ethylene and diethyl ether produced in the platinum section can be attributed to the presence of acid sites on the Al_2O_3 monoliths, however, dehydration reactions primarily occurred in the zeolite

layer. The mechanism of ethanol dehydration over zeolitic catalysts involves unimolecular and bimolecular dehydration steps that result in synthesis of ethylene and diethyl ether, respectively. Ethylene is the dominant dehydration product in the zeolite layer due to the operating temperatures of the zeolite. High temperatures and small pore size materials preferentially result in synthesis of ethylene as reported by Hsu et al.[37,38]

2.4.2 Isothermal Ethanol Conversion Experiments

An isothermal experiment at the same total flow condition using the same zeolite catalysts was performed to evaluate ethanol dehydration over HZSM-5 zeolite catalysts independent of ethanol decomposition reactions that occur during autothermal experiments.

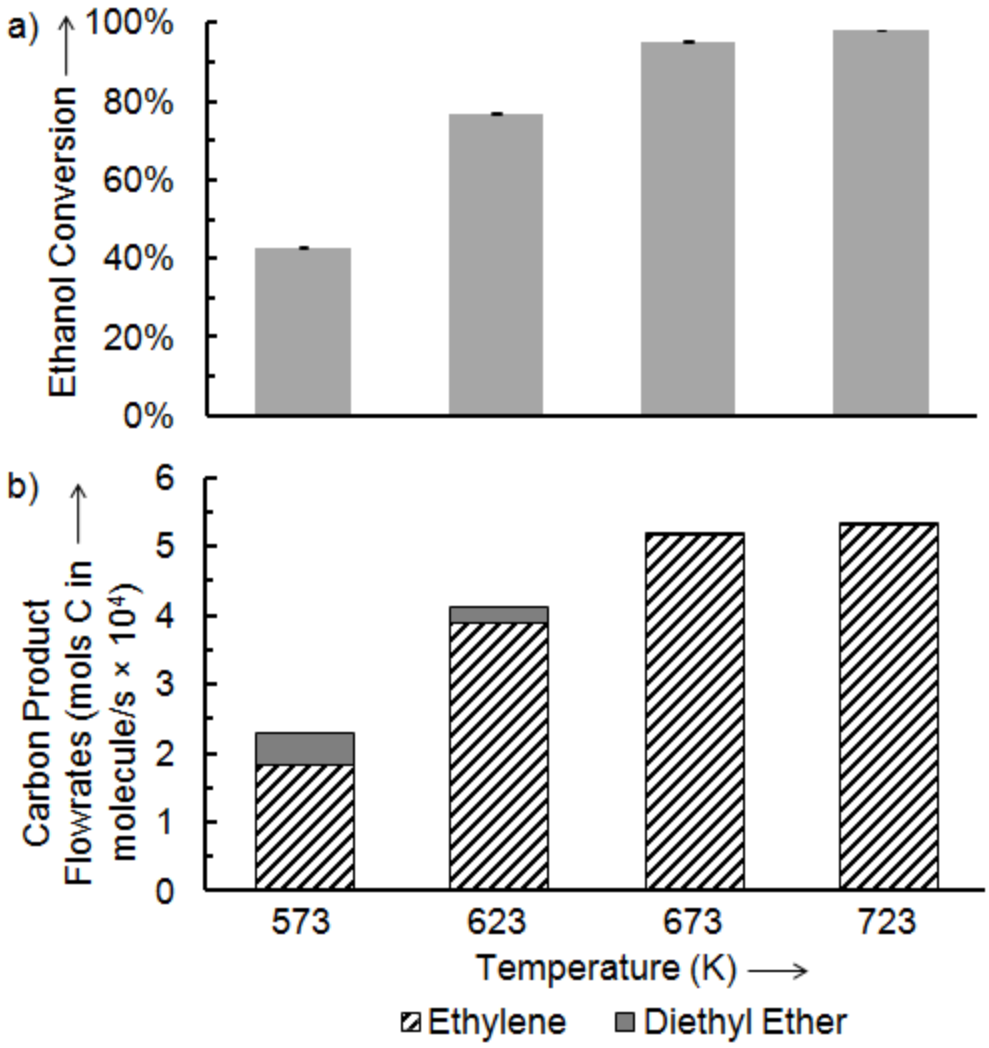

Figure 2.3 a) Isothermal ethanol conversion on HZSM-5 coated Al_2O_3 monolith catalysts. Error bars on the ethanol conversion chart represent the 95% confidence interval. b) Carbon product flow rates. Diethyl Ether (dark gray), Ethylene (right slash). The total overall input into the reactor was maintained at 50 cm^3/s standard conditions. Ethanol was pumped as a liquid at 1.53×10^{-2} cm^3/s and fed to the reactor through a nebulizer. Each of the four Al_2O_3 monoliths was coated with approximately 200 mg of H-ZSM-5. The zeolite catalyst maintained operation at a steady state over the 1 hour duration for sampling under isothermal conditions.

As expected, with increasing reactor temperatures in the zeolite layer, the yield of the unimolecular dehydration product, ethylene, increased faster than the yield of the bimolecular dehydration product, diethyl ether.[38] While zeolite product distributions remained similar between the isothermal and autothermal experiments, the overall conversion of ethanol in the zeolite layer was significantly higher during isothermal

experiments than that observed during autothermal experiments for similar temperature ranges of operation. As seen in figure 2.3, at an isothermal temperature of 623 K, over 75% of ethanol was dehydrated by the zeolite catalyst to ethylene and diethyl ether in a contact time of 70 milliseconds. A similar overall ethanol conversion was achieved in the autothermal reactor at E: H: O ratios of 2.1: 2: 1 and 1.7: 2: 1 which resulted in middle zeolite temperatures of 710 and 778 K respectively. However, only 39% and 32% of the ethanol was converted in the zeolite section, the remainder coming from ethanol decomposition and oxidation in the noble metal section. At isothermal temperatures of 673 and 723 K, over 95% of the ethanol was dehydrated. During autothermal experiments, at least 25% of the ethanol remained unconverted at similar temperatures.

There are two explanations for why ethanol conversion was higher in the isothermal experiments at similar temperatures: the temperature profile in the zeolite layer was different between the two set of experiments, and large quantities of acetaldehyde were present in the autothermal experiments but not in the isothermal experiments The temperature profile of the reactor was uniform in the isothermal experiments due to constant heat input from the tube furnace along the length of the reactor. In contrast, the temperature profile in the autothermal experiments varied by as much as 130 K from the top zeolite monolith to the bottom zeolite monolith which makes a direct comparison of autothermal and isothermal results difficult.

In the isothermal experiment, no ethanol decomposition products were present to competitively adsorb on the acid sites and act as coke precursors, thus allowing for higher ethylene conversion than in the autothermal experiments. The only C_2 compound present other than ethanol in the autothermal experiments is acetaldehyde.

To examine the effect of acetaldehyde on the H-ZSM-5 coated monoliths, the isothermal experiments were repeated with a 15 mol% feed of acetaldehyde in ethanol, the results of which are shown in figure 2.4.

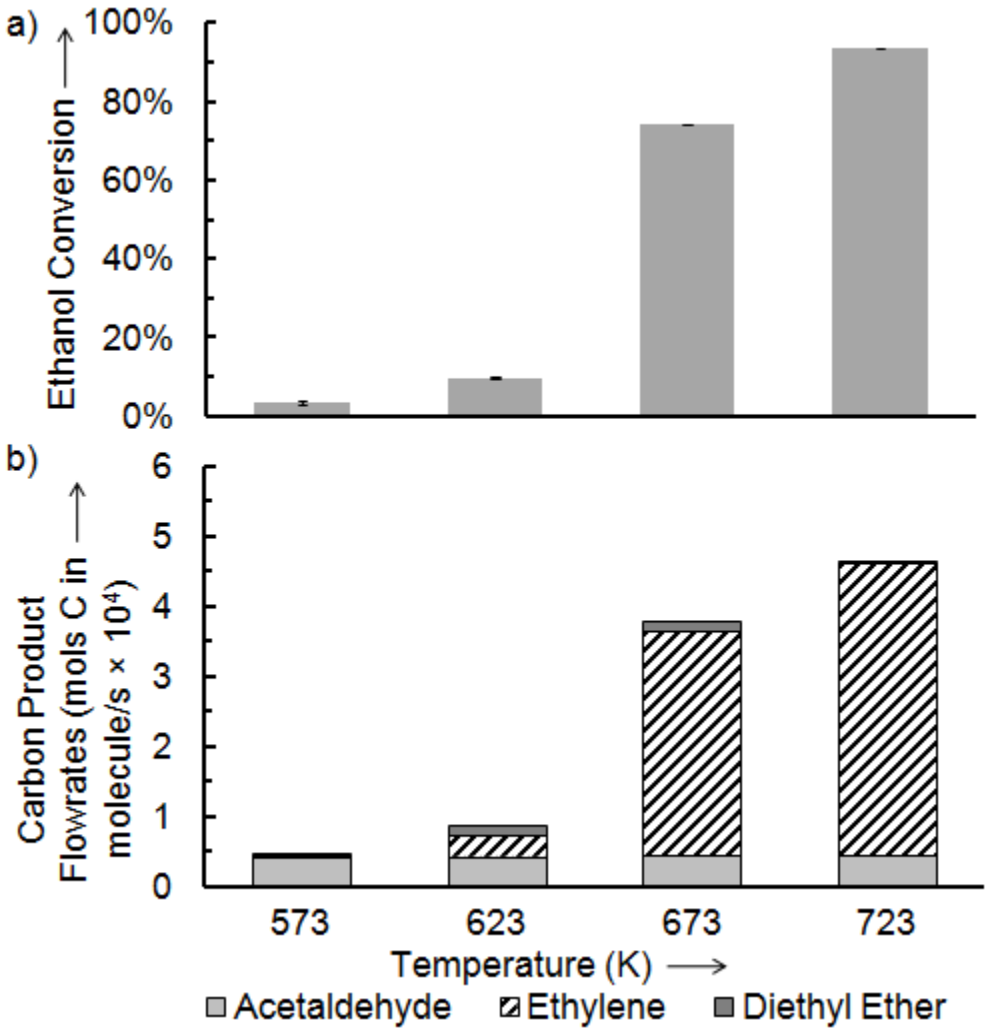

Figure 2.4 a) Isothermal ethanol conversion on HZSM-5 coated Al_2O_3 monolith catalysts. Error bars on the ethanol conversion chart represent the 95% confidence interval. b) Carbon product flow rates. Diethyl Ether (dark gray), Ethylene (right slash), Acetaldehyde (light gray). The total overall input into the reactor was maintained at 50 cm^3/s standard conditions. A mixture of 85 mol% ethanol and 15 mol% acetaldehyde was pumped as a liquid at 1.53×10^{-2} cm^3/s and fed to the reactor through a nebulizer. Each of the four Al_2O_3 monoliths was coated with approximately 200 mg of H-ZSM-5. The zeolite maintained operation at a steady state over the 1 hour duration for sampling under isothermal conditions.

There was a noticeable decrease in total ethanol conversion over the zeolite catalysts when acetaldehyde was co-fed. At 673 K, the ethanol conversion dropped by

20% while at 623K the total ethanol conversion decreased over 60% with the acetaldehyde co-feed compared to a pure ethanol feed. Diaz et al. identified oligomeric species in H-ZSM-5 by fourier transmission infrared spectroscopy (FTIR) when acetaldehyde was exposed to H-ZSM-5 at 313 K and acetaldehyde pressures over 400 Pa.[39] We surmise that inhibition by acetaldehyde in autothermal experiments results in lower ethanol conversion at similar temperatures compared to isothermal experiments due to the formation of oligomeric species which inhibit ethanol conversion.

To prevent acetaldehyde formation, an autothermal reactor was setup with a methane feed upstream of the noble metal layer and an ethanol side feed downstream of the noble metal layer. This series ethanol feed design allows the partial oxidation of a sacrificial fuel to provide the heat necessary to drive dehydration reactions downstream in the zeolite layer while eliminating catalytic degradation of ethanol over the metal catalyst. Additionally, homogeneous ethanol degradation is reduced because the ethanol does not flow past the hottest part of the reactor. As shown in figure 2.5, this reactor was capable of dehydrating over 90% of the ethanol fed into the system and selectively producing ethylene.

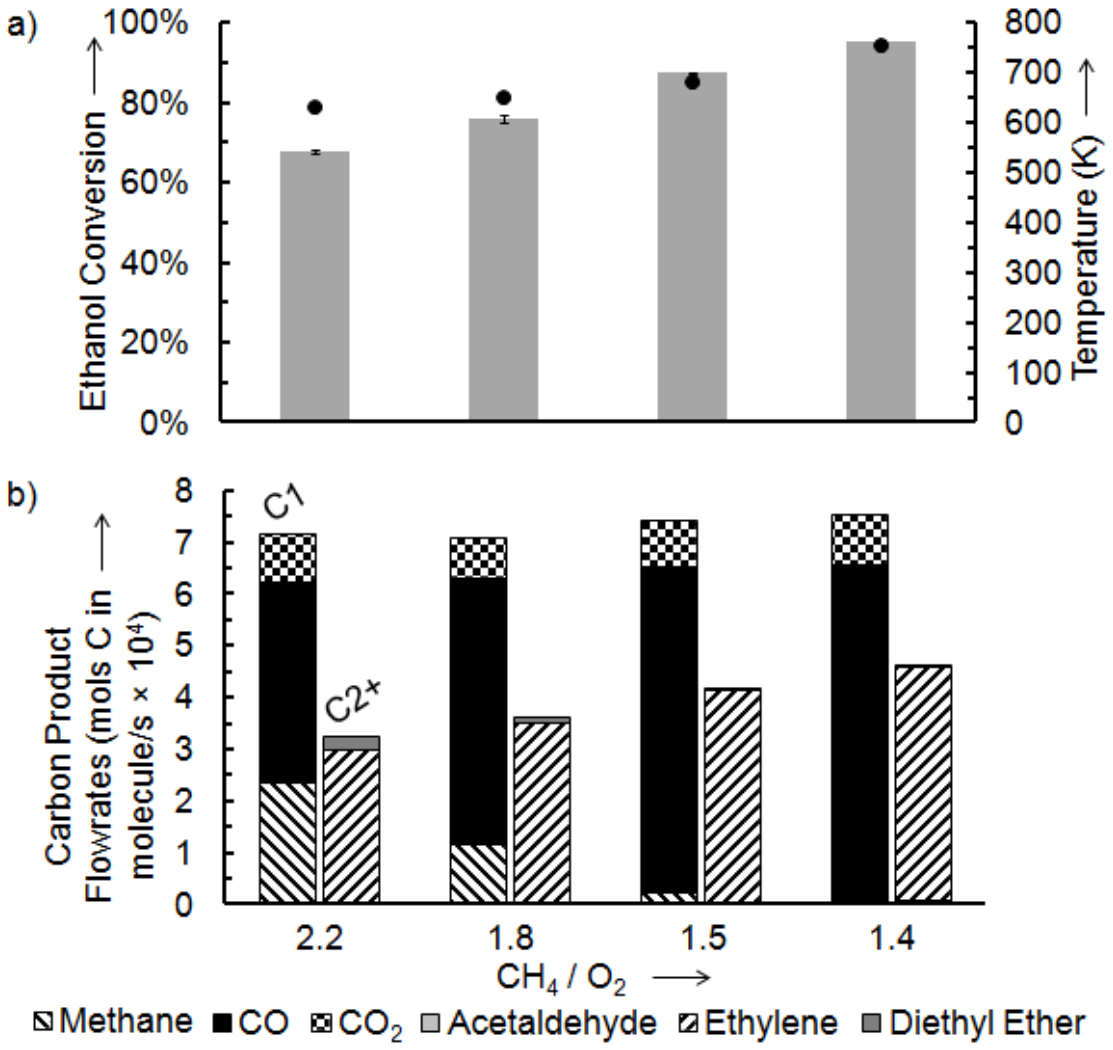

Figure 2.5. a) Autothermal ethanol conversion in the stratified reactor with a methane feed upstream and an ethanol side feed. Error bars on the ethanol conversion chart represent the 95% confidence interval. The temperature shown is for the middle zeolite-coated monolith. Post-Zeolite Conversion (dark gray), Zeolite Temperature (black circle). b) Carbon product flow rates grouped into molecules containing a single carbon atom (C1) and molecules containing two or more carbon atoms (C2+). Diethyl Ether (dark gray), Ethylene (right slash), Acetaldehyde (light gray), CO_2 (checkered), CO (black), Methane (left slash). The total overall input into the reactor was maintained at 50 cm^3/s standard conditions. Ethanol was pumped as a liquid at 1.53×10^{-2} cm^3/s and prevaporized before entering the reactor. The noble metal section contained approximately 20 mg of platinum coated on Al_2O_3 beads. Each of the four Al_2O_3 monoliths in the zeolite section was coated with approximately 200 mg of H-ZSM-5. The zeolite and noble metal catalyst maintained operation at a steady state over the 1 hour duration for sampling under autothermal conditions.

As shown in the parallel ethanol feed autothermal reactor (Figure 2.2), C1 products are only formed in the noble metal layer and pass through the zeolite layer without reacting. In the series ethanol feed reactor, again all C1 products (carbon monoxide, carbon dioxide) are the result of catalytic partial oxidation in the platinum

layer. As the CH_4/O_2 ratio changes, the C1 product selectivities change, however, the sum of all the carbon in C1 molecules (CO, CO_2, CH_4) is equal to the total amount of carbon in the methane feed.

The methane to oxygen ratio was maintained at fuel rich conditions and all oxygen was consumed for all CH_4/O_2 ratios examined. As the oxygen feed increased, the CH_4/O_2 ratio decreased and the reactor temperature increased due to the increasing amount of methane partial oxidation. From figure 2.5, it can be seen that 32% of methane passed through unconverted at a CH_4/O_2 of 2.2 while at a CH_4/O_2 of 1.4, less than 1% of methane remained unconverted which resulted in a concomitant increase in the amount of CO produced. These results are consistent with those presented by Hickman et al. who examined methane catalytic partial oxidation over 10-12% wt Pt coated alumina monoliths in air mixtures at 4 SLPM in 10 ms contact times, and found that as the CH_4/O_2 ratio decreased from 2 to 1, the CO selectivity increased from 85 to 90% and the methane conversion increased from 50 to 90%.[17]

The middle zeolite temperature in the series ethanol feed reactor ranged from 623 to 720 K, which is similar to the middle zeolite temperatures for the four lowest E:H:O ratios in the parallel ethanol feed reactor. Although operating at similar temperature regimes, the series ethanol feed reactor had both higher total ethanol conversions (68-95% vs. 57-74%) and twice as much ethylene production than the parallel feed reactor. This is due to the ethanol side feed not coming into contact with the noble metal layer, which eliminated ethanol C-C decomposition and combustion steps.

The sum of all carbon in C2+ products (ethylene, diethyl ether, and acetaldehyde) and unconverted ethanol is equal to the total amount of carbon in the ethanol feed,

indicating that ethanol did not decompose into smaller C1 products. At a CH_4/O_2 ratio of 1.4, the highest autothermal conversion of ethanol, 95%, occurred in the series ethanol feed reactor, yet less than 5% of ethanol was converted to acetaldehyde. At all other CH_4/O_2 ratios examined, less than 1% of ethanol was converted to acetaldehyde In the parallel ethanol feed reactor operating at similar zeolite temperature conditions, between 10-35% of ethanol was converted to acetaldehyde over the noble metal layer.

These results demonstrate that a zeolite layer can be integrated downstream in a millisecond contact time reactor to achieve autothermal steady state ethanol dehydration. Reed used the Diebold kinetic model to show that heat flux requirements greater than 100 W/cm^2 are necessary to prevent char and tar formation during biomass decomposition.[9,12] Dauenhauer has demonstrated that heat flux rates over 300 W/cm^2 are possible when cellulose particles are directly impinged on porous supports, such as those used in short contact time reactors.[23] To maintain such high heating rates, fuel contact times with the noble metal in the millisecond contact time range must be maintained.[19]

In industrial petroleum refinery settings, such as fluid catalytic cracking units, zeolites routinely operate in 2 second residence time conditions, which is at least an order of magnitude beyond that allowed to process biomass to minimize side products. This research demonstrates that it is possible to incorporate zeolites into a reactor with sub-one-second time scales. The stratified partial oxidation reactor presented serves as a demonstration unit for a next generation biomass to biofuel reactor capable of the decomposition and deoxygenation steps necessary to create a biofuel suitable for direct substitution as a transportation fuel. Stratified partial oxidation reactors can perform

these transformation steps without any additional process heat and in millisecond contact times.

2.5 Conclusions

Using a stratified autothermal short contact time reactor, ethanol was dehydrated to ethylene. Decreasing the E: H: O ratio by increasing hydrogen and oxygen flow resulted in higher operating temperatures and larger conversions of ethanol in both the platinum layer and zeolite layer. Over 50% of the ethanol remaining after the noble metal layer was dehydrated in the zeolite layer using an ethanol-hydrogen parallel co-feed reactor. Isothermal experiments using an H-ZSM-5 catalyst achieved over 99% conversion of ethanol to dehydration products in 50-80 millisecond contact times. Acetaldehyde produced in the platinum layer of the reactor led to a decrease in ethanol dehydration conversion in the zeolite layer compared to isothermal ethanol dehydration reactions using the same catalyst. An ethanol-methane series co-feed reactor configuration achieved over 95% conversion of ethanol while less than 5% of the ethanol was converted to acetaldehyde. The high rate of ethanol conversion to ethylene in both autothermal and isothermal reactors demonstrates that zeolite catalysts can be incorporated into millisecond contact time reactors to perform deoxygenation reactions.

Chapter 3

Future Directions

The initial experiments only examined one pyrolysis oil model compound, ethanol. The surrogate feed should be expanded in future experiments to include other alcohols, phenols, aldehydes, ketones, acids, and other compounds found in pyrolysis oil so that key catalyst and reactor parameters can be identified in order to maximize oxygen removal while limiting catalyst deactivation and side product formation. Finally, solid feedstock feeding using lignocellulosic fuels should be examined. In addition to expanding into other surrogate feeds, the following three areas warrant investigation.

3.1 Mesoporous Zeolites

Zeolite structures designed to have mesoporous channels need to be studied to examine solutions to possible diffusion limitations in the zeolite layer of the short contact time reactor. Optimal zeolite catalyst design results from a balance of increasing mesoporous channels, which allow for high rates of diffusion, while maintaining a high amount of nanoporous volume to perform the shape selective catalysis. MCM-22 is a two-dimensional framework containing 10 T-atom channels that can be calcined to form a layered zeolite material with large supercages. If alumina or silica pillars are introduced into the material, the layers can be separated, allowing for a mesoporous interlayer channel infrastructure to form instead of the large supercages. This new structure is referred to as MCM-36.[40] The mesoporous infrastructure should allow for faster diffusion through the zeolite, so that more of the zeolite crystal will be available to

perform catalytic chemistry. Conversion rates on a per weight catalyst basis will be examined for MCM-22 and MCM-36 deposited zeolite monoliths. In additional to a higher conversion, the selectivity to bimolecular products is expected to increase with MCM-36 due to the relative higher increase in diffusion rates for larger compared to smaller products.

3.2 Spatial Profiling

The Schmidt group has developed a spatial profiling technique where a fused silica capillary is directed through a 0.75mm pre-drilled channel through the center of foam catalyst. Measurement devices inserted into the capillary can be moved in sub-mm increments by use of a stepper motor. This spatial profiling technique allows for sub-mm resolution of gas temperature, catalyst surface temperature, and gas composition along the axis of the reactor.[41]

A thermocouple can be inserted into the capillary allowing for gas temperature measurement. Radiation generated from the monolith is used to measure catalyst surface temperature by an optical pyrometer. Gas composition is determined by creating a 0.3 mm sampling orifice into the side of the capillary and drawing effluent by high vacuum to a GC-MS.

Spatial profiling will allow us to identify an oxidation zone where partial oxidation of sacrificial fuel and model biomass components occurs and a reforming zone where water gas shift, steam reforming, and catalytic decomposition of model compounds occur. A short catalyst bed will not have enough catalyst for significant oxidation to occur, while a longer catalyst bed will have additional reforming and

catalytic decomposition capabilities. Spatial profiling will allow us to determine the optimal length of the catalyst bed by examining gas composition and temperature. We will be able to identify the exact length of catalyst bed where heat generation is enough to ensure a high temperature zone in the zeolites while minimizing side product formation.

In the zeolite portion, spatial profiling can be used to verify kinetic parameters. Similar isothermal experiments described in the experimental section can be performed, but this time sampling composition along the length of the catalyst, which will provide a more accurate measurement of ethanol partial pressure vs. diethyl ether and ethylene flowrates. The current experimental section represents only the inlet partial pressure of ethanol and product compositions averaged over the length of the bed. With spatial sampling measurements, we can measure the model compound partial pressure drop along the axis of the reactor and the corresponding expected decrease in product formation.

3.3 Advanced Stratification Setups: Hydrogen Transfer and Carbon Bond Formation

After breaking down biomass and removing oxygen, chain growth steps are needed to build molecules large enough to be used as a transportation fuel. One of the benefits of a stratified system is the ability to use multiple different types of zeolite throughout the length of the reactor. It would be unrealistic to assume that a single zeolite type will be the best choice for dehydration, chain growth, and hydrogen transfer. Due to the sequential nature of the reactions involved in fuel formation, an optimal zeolite can be used for each step involved.

Every oxygen atom removed by a dehydration reaction consumes two hydrogen atoms. To convert biomass model compounds to transportation fuels, the carbon to hydrogen ratio of the product needs to be maintained at the level of those found in alkanes . In order for this to occur, hydrogen must be incorporated into the product. Alkanes can serve as a cheap source of hydrogen. A bifunctional catalyst capable of activating methane and forming aromatics from olefins and paraffins will be placed downstream of the initial HZSM-5 layer.[42] Methane will be fed into the reactor before the Mo/HZSM-5 catalyst. The reactor effluent will be examined by GC-MS for aromatic compounds as well as methane consumption.

Bibliography

1. Renewable Fuels Association. 2009 ethanol production exceeds 10.7 billion gallons. *Corn and Soybean Digest* Mar. 1, 2010.
2. National Renewable Energy Laboratory Report. Integrated biorefinery research facility: advancing biofuels technology. Report No. FS-510-44997, March 2009.
3. S.D. Phillips. Technoeconomic analysis of a lignocellulosic biomass indirect gasification process to make ethanol via mixed alcohols synthesis. *Industrial & Engineering Chemistry Research*, 46:8887-8897, 2007.
4. A. Dutta and S.D. Phillips. Thermochemical ethanol via direct gasification and mixed alcohol synthesis of lignocellulosic biomass. *National Renewable Energy Lab Technical Report*, July 2009.
5. L. Tao and A. Aden. The economics of current and future biofuels. *In Vitro Cellular & Developmental Biology – Plant*, 45:199-217, 2009.
6. R.E.H. Sims, A. Hastings, B. Schlamadinger, G. Taylor, and P. Smith. Energy crops: current status and future prospects. *Global Change Biology*, 12:2054-2076, 2006.
7. A. Demirbas. The influence of temperature on the yields of compounds existing in bio-oils obtained from biomass samples via pyrolysis. *Fuel Processing Technology*, 88:591-597, 2007.
8. R. French and S. Czernik. Catalytic pyrolysis of biomass for biofuels production. *Fuel Processing Technology*, 91:25-32, 2010.
9. A.V. Bridgewater, D. Meier, and D. Radlein. An overview of fast pyrolysis of biomass. *Organic Geochemistry*, 30:1479-1493, 1999.

10. S. Czernik and A.V. Bridgwater. Overview of applications of biomass fast pyrolysis oil. *Energy & Fuels*, 18:590-598, 2004.
11. M. Balat, M. Balat, E. Kirtay, H. Balat. Main routes for the thermo-conversion of biomass into fuels and chemicals. *Energy Conversion and Management*, 50:3147-3157, 2009.
12. T.B. Reed and C.D. Cowdery. Heat flux requirements for fast pyrolysis and a new method for generating biomass vapor. *American Chemical Society Spring Symposium,* 32:68-81, 1987.
13. T.A. Milne, R.J. Evans, and N. Nagle. Catalytic conversion of microalgae and vegetable oils to premium gasoline, with shape-selective zeolites. *Biomass*, 21:219-232, 1990.
14. J. Diebold and J. Scahill. Biomass to gasoline (BTG): Upgrading pyrolysis vapors to aromatic gasoline with zeolite catalysis at atmorspheric pressure. *ACS Symposium Series*, 376:297-307, 1988.
15. T.A. Milne and R.J. Evans. Molecular characterization of the pyrolysis of biomass. 1. Fundamentals. *Energy and Fuels*, 1:123-137, 1987.
16. Diebold and J. Scahill. Production of primary pyrolysis oils in a vortex reactor. *ACS Symposium Series*, 376:31-40, 1988.
17. D.A. Hickman and L.D. Schmidt. Production of syngas by direct catalytic oxidation of methane. *Science*, 259:343-346, 1993.
18. D.C. Rennard, J.S. Kruger, and L.D. Schmidt. Autothermal catalytic partial oxidation of glycerol to syngas and to non-equilibrium products. *ChemSusChem,* 2:89-98, 2009.

19. J. L. Colby, P. J. Dauenhauer, and L. D. Schmidt. Millisecond autothermal steam reforming of cellulose for synthetic biofuels by reactive flash volatilization. *Green Chemistry*, 10:773-783, 2008.
20. P.M. Torniainen, X. Chu, and L.D. Schmidt. Comparison of monolith-supported metals for the direct oxidation of methane to syngas. *Journal of Catalysis,* 146:1-10, 1994.
21. M. Huff, S.S. Bharadwaj, and L.D. Schmidt. Catalytic partial oxidation reactions and reactors. *Chemical Engineering Science,* 49:3981-3994, 1994.
22. A. Dietz III and L.D. Schmidt. Monoliths for partial oxidation catalysis. *MRS Proceedings,* 368:299-307, 1995.
23. P.J. Dauenhauer, J.L. Colby, C.M. Balonek, W.J. Suszynski, and L.D. Schmidt. Reactive boiling of cellulose for integrated catalysis through an intermediate liquid. *Green Chemistry*, 11:1555-1561, 2009.
24. A. Corma. State of the art and future challenges of zeolites as catalysts. Journal of Catalysis, 216:298-312, 2003.
25. A.C. Caputo, M. Palumbo, P.M. Pelagagge, and F. Scacchia. Economics of biomass energy utilization in combustion and gasification plants: effects of logistic variables. *Biomass and Bioenergy*, 28:35-51, 2005.
26. P.J. Dauenhauer, B.J. Dreyer, N.J. Degenstein, and L.D. Schmidt. Millisecond reforming of solid biomass for sustainable fuels. *Angewandte Chemie*, 46:5864-5867, 2007.

27. D.C. Rennard, P.J. Dauenhauer, S.A. Tupy, and L.D. Schmidt. Autothermal catalytic partial oxidation of bio-oil functional groups: esters and acids. *Energy & Fuels,* 22:1318-1327, 2008.

28. C. Wheeler, A. Jhalani, E.J. Klein, S. Tummala, and L.D. Schmidt. The water-gas-shift reaction at short contact times. *Journal of Catalysis*, 223:191-199, 2004.

29. A.G. Gayubo, A.T. Aguayo, A. Atutxa, R. Aguado, and J. Bilbao. Transformation of oxygenate components of biomass pyroysis oil on a HZSM-5 zeolite. I. alcohols and phenols. *Industrial & Engineering Chemistry Research*, 43:2610-2618, 2004.

30. G.J. Panuccio and L.D. Schmidt. Increasing olefins by H_2 and CH_4 addition to the catalytic partial oxidation of n-octane. *Applied Catalysis A: General*, 313:63-73, 2006.

31. A.S. Bodke, D. Henning, L.D. Schmidt, S.S. Bharadwaj, J.J. Maj, and J. Siddall. Oxidative dehydrogenation of ethane at millisecond contact times: effect of H_2 addition. *Journal of Catalysis*, 191:62-74, 2000.

32. J.R. Salge, G.A. Deluga, and L.D. Schmidt. Catalytic partial oxidation of ethanol over noble metal catalysts. *Journal of Catalysis*, 235:69-78, 2005

33. A.F. Lee, D.E. Gawthrope, N.J. Hart, and K. Wilson. A fast XPS study of the surface chemistry of ethanol over Pt { 1 1 1 }. *Surface Sciences*, 548:200-208, 2004.

34. B.L.M. Hendriksen and J.W.M. Frenken. CO Oxidation on Pt(110): scanning tunneling microscopy inside a high-pressure flow reactor. *Physical Review Letters*, 89, 2002.

35. I. Langmuir. The mechanism of the catalytic action of platinum in the reactions $2CO + O_2 = 2CO_2$ and $2H_2 + O_2 = 2H_2O$. *Transactions of the Faraday Society*, 17:621-654, 1922.

36. J.M. White and A. Golchet. A transient kinetics study of the reaction of CO with chemisorbed oxygen on platinum. *The Journal of Chemical Physics*, 66:5744-5748, 1977.

37. H. Chiang and A. Bhan. Catalytic consequences of hydroxyl group location on the rate and mechanism of parallel dehydration reactions of ethanol over acidic zeolites. *Journal of Catalysis*, 271:251-261, 2010.

38. D.E. Bryant and W.L. Kranich. Dehydration of alcohols over zeolite catalysts. *Journal of Catalysis,* 8:8-13, 1967.

39. C.D.C. Diaz, S. Locatelli, and E.E. Gonzo. Acetaldehyde adsorption on HZSM-5 studied by infrared spectroscopy. *Zeolites*, 12:851-857, 1992.

40. S. Mahehwari, C. Martinez, M. Portilla, F. Llopis, A. Corma, and M. Tsapatsis. Influence of layer structure preservation on the catalytic properties of the pillared zeolite MCM-36. *Journal of Catalysis*, 272:298-308, 2010.

41. R. Horn, N.J. Degenstein, K.A. Williams, and L.D. Schmidt. Spatial and temporal profiles in millisecond partial oxidation processes. *Catalysis Letters,* 110:169, 2006.

42. Y.H. Kim, R.W. Borry III, and E. Iglesia. Genesis of methane activation sites in Mo-exchanged H-ZSM-5 catalysts. *Microporous and Mesoporous Materials*, 35:495-509, 200.

43. PP.E.A. de Moor, T.P.M. Beelen, R.A. van Santen, L.W. Beck, M.E. Davis. Si-MFI crystallization using a “dimer” and “trimer” of TPA studied with small-angle X-ray *Scattering. Journal of Physical Chemistry B*, 104:7600-7611, 2000.

Appendix A Autothermal temperature profiles and reactor schematics

Ethanol: Hydrogen: Oxygen	6.4: 2: 1	3.8: 2: 1	3.2: 2: 1	2.7: 2: 1	2.1: 2: 1	1.7: 2: 1
Top	537	633	680	705	775	844
Mid-Top	522	608	642	661	725	795
Middle	518	599	633	650	710	778
Mid-Bottom	510	589	620	638	695	759
Bottom	497	568	594	611	660	713

Table A.1 Recorded temperatures (K) during autothermal ethanol conversion for the zeolite layer in the ethanol, hydrogen co-fed reactor.

CH_4/O_2	2.2	1.8	1.5	1.4
Ethanol Feed	806	851	907	1022
Top	705	734	784	879
Mid-Top	679	707	749	828
Middle	630	649	682	756
Mid-Bottom	604	622	653	731
Bottom	590	606	638	714

Table A.2 Recorded temperatures (K) during autothermal ethanol conversion for the zeolite layer and ethanol entrance temperature for the methane fed reactor with ethanol side feed addition.

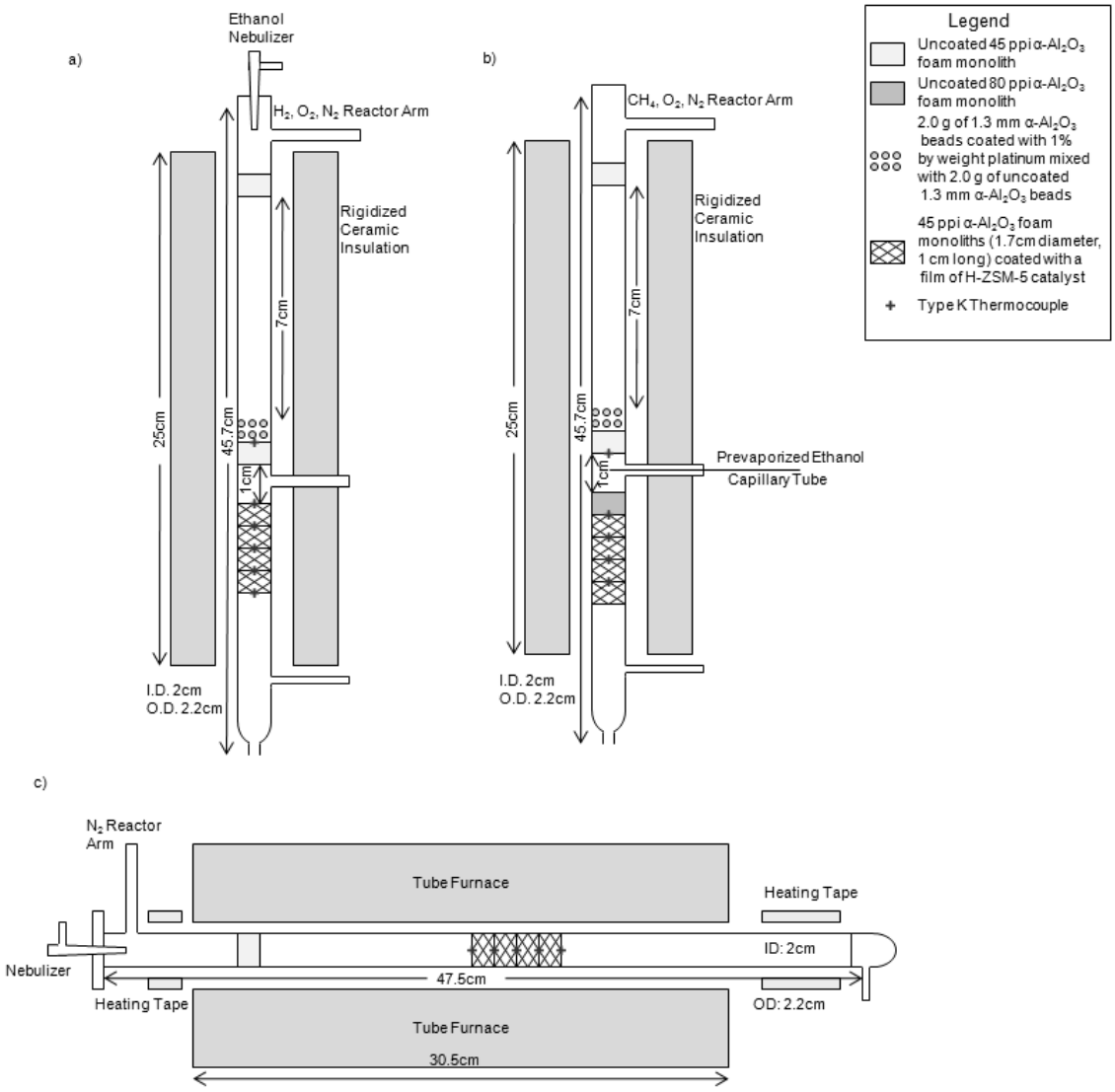

Figure A.3 Autothermal stratified reactor using a) an ethanol-hydrogen co-feed, b) a methane feed upstream and an ethanol side feed, and c) an isothermal reactor.

Appendix B Zeolite Synthesis

Silicalite-1 seeds were synthesized using the method of de Moor.[43] Silicic acid (2.5 g) was dissolved into a solution made with 7.29g TPAOH (1M) and NaOH(10M) 282 μl by heating at 363 K for 2 hours with a composition of 2.4 TPAOH:0.44Na_2O:10SiO_2:114H_2O. After the solution became clear, it was transferred into a Teflon container and heated at 423 K for 24 hours. The synthesized silicalite-1 crystals solution were centrifuged at 10000 rpm for 10 min and re-dispersed in DI water. The process was repeated until the pH of the solution was down to 7. In order to check the weight concentration of the solution, 3 ml of the solution was dried at 383 K and the final product was weighed. DI water added to adjust the final concentration to 4.6wt% silicalite-1 crystals. The pH of the silicalite-1 nanocrystals solution was adjusted to 9.5-10.0 by the addition of a 0.10 M NH_3 solution.

The surface of the monoliths was cleaned at room temperature in acetone for 10 min under ultrasonication and, then, for 10 min in a solution with the following composition (volume parts): 5H_2O:H_2O_2:HCl (H_2O_2: 30% in water and HCl: 37%). Between the cleaning procedures, the support was rinsed by DI water. The supports were treated for 1 hour in 1wt % PDDA cationic polymer solution. The pH of the polymer solution was adjusted to 8 by using a 0.10 M NH_4OH solution. The supports were rinsed with 0.10 M NH_4OH solution four times to remove the excess polymer. The charge-reversed support was treated in 4.6 wt% silicalite-1 solution for 1 h, then was rinsed with 0.10 M NH_4OH solution four times.

The seed-coated supports were transferred to 8 ml zeolite synthesis solution made with the composition of 3TPAOH:25SiO_2:0.25 Al_2O_3:1.0Na_2O:1450H_2O. The detailed procedure is described: 0.082g aluminum isopropoxide was dissolved into a SDA

solution made by mixing 2.42 g TPAOH(1M), 160 ul NaOH (10M), 18.94g DI H_2O. After the solution became completely clear, 4.16 g TEOS was added and aged for 12 hours with stirring. After 12 h, the TEOS was completely hydrolyzed, and the solution was clear.

The seeded growth was performed at 423 K for 48 hours. The zeolite coated supports were rinsed with DI water four times and dried at 343 K for 12 hours.

After treatment in flowing dry air at 823 K for 24 hours (1 K/min), the zeolite coated supports were ion-exchange 3 times in 1M NH_4NO_3 solution at 373 K for 1 h. Finally, the supports were calcined again at 823 K for 24 hours to form H-type zeolite coated supports.